Analysis of the dust jet imaged by *Rosetta* VIRTIS-M in the coma of comet 67P/Churyumov–Gerasimenko on 2015 April 12

V. Tenishev,[1]★ N. Fougere,[1] D. Borovikov,[1] M. R. Combi,[1] A. Bieler,[1]
K. C. Hansen,[1] T. I. Gombosi,[1] A. Migliorini,[2] F. Capaccioni,[2]
G. Rinaldi,[2] G. Filacchione,[2] L. Kolokolova[3] and U. Fink[4]

[1]*Department of Climate and Space Sciences and Engineering, University of Michigan, Ann Arbor, MI 48109, USA*
[2]*INAF Istituto di Astrofisica e Planetologia Spaziali, I-00133 Rome, Italy*
[3]*Astronomy Department, University of Maryland, College Park, MD 20742, USA*
[4]*Lunar and Planetary Laboratory, University of Arizona, Tucson, AZ 85721, USA*

ABSTRACT

This work is a part of a more global effort aimed at understanding and interpreting *in situ* and remote sensing data acquired by instruments on board *Rosetta*. This study aims at deriving the dust mass source rate and the location of the dust jet source observed by *Rosetta* VIRTIS-M on 2015 April 12. The analysis is performed by means of the coupled kinetic modelling of gas and dust in the coma of comet 67P/Churyumov–Gerasimenko, which were used for calculating the coma brightness as it would be seen from the *Rosetta* spacecraft. The dust mass production rate and a possible location of the jet origin needed to explain the *Rosetta* VIRTIS-M dust brightness image were inferred by comparing the calculated brightness with VIRTIS-M data. Our analysis suggests that the dust mass production rate needed to maintain the observed jet is about 1.9 kg s^{-1}. According to our analysis, the location of the observed jet surface footprint is outside of the nucleus area characterized by the highest gas production rate, which suggests that gas and dust source rates are not necessarily proportional to each other across the entire nucleus surface. The inferred location of the possible jet origin is consistent with that of the observed active pits. In this paper, we show that the jet intensity is variable in time, and has a lifetime of at least 10 h.

Key words: comets: general – comets: individual: 67P/Churyumov–Gerasimenko.

1 INTRODUCTION

A cometary coma is a complex and mutually interconnected system that consists of neutral gas and corresponding ions, cometary dust, and plasma of solar wind. Due to the negligible gravity of a comet's nucleus, a coma has a characteristic size that by many orders of magnitude exceeds that of the nucleus. Such an extended dusty gas cloud is affected mainly by molecular collisions, radiation cooling, and photolytic, charge-exchange, and impact-ionization reactions (Bockelée-Morvan & Crovisier 1987; Combi & Smyth 1988; Combi 1996).

Comet 67P/Churyumov–Gerasimenko is the target of the *Rosetta* mission, which is the first mission that escorts a comet along its way through the Solar system for an extended amount of time. The list of the main scientific objectives of the mission includes the global characterization of the comet's nucleus, determination of the surface composition, and a study of the comet's activity development. To achieve these goals, the orbiter carries a suite of 11 instruments for the *in situ* and remote-sensing observation of dust and gas that make up the comet's coma.

Dust images delivered by *Rosetta* provide one of the most important opportunities to characterize the temporal and spatial variability of the dust population in a cometary coma. Analysis of these images could improve the understanding of the physical mechanisms that produce dust jets, uncover a relation between gas and dust activities, and constrain a size distribution of the dust particles.

In this paper, we present results of our analysis of the dust jet observed by the mapping channel of the *Rosetta* Visible and InfraRed Thermal Imaging Spectrometer (VIRTIS) on 2015 April 12, and a comparison of the model results with the coma dust brightness imaged by VIRTIS-M between 2015 April 11 and 13 (Migliorini et al. 2016). One of the main advantages of using these images of a jet is that we already have a multi-instrument verified description of the gas environment for that time (Fougere et al. 2016). In this paper, we discuss the important implications on the dust and gas activity,

★ E-mail: vtenishe@umich.edu

and their distributions on the surface inferred from the VIRTIS-M images with our dusty gas kinetic model of a cometary coma.

2 DUST IN THE COMA OF COMET 67P/CHURYUMOV–GERASIMENKO

Dust and gas are two primary components of a cometary coma. Remote-sensing instruments on board *Rosetta* (e.g. OSIRIS and VIRTIS) provide an unprecedented opportunity to observe cometary dust. Some of these observations are already detailed by, for example, Lara et al. (2015), Lin et al. (2015), and Schulz et al. (2015), and summarized by Rotundi et al. (2015), who have suggested the dust-to-gas mass ratio of 4 ± 2, the differential size distribution power index of -4, and the dust-loss rate of $7 \pm 1 \, \mathrm{kg \, s^{-1}}$ at heliocentric distances of $3.4 - 3.6$ au.

Dust particles observed by *Rosetta* so far fall into two major categories: compact (diameter of 0.03–1 mm) and fluffy (diameter 0.2–2.5 mm) (e.g. Della Corte et al. 2015; Rotundi et al. 2015). Even though large in size, fluffy dust particles provide a negligible contribution to the total dust mass ejection rate (Fulle et al. 2015b,a). A mechanism for the fluffy particle formation was investigated by, for example, Skorov & Blum (2012).

Smaller size particles, charged nanograins, were detected by the Ion and Electron Sensor on board *Rosetta* at cometocentric distances of 50–65 km (Burch et al. 2015). Charging of these nanograins is dominated by photoemission, electron collection, and secondary electron emission currents.

Most of the compact particles observed by the Grain Impact Analyser and Dust Accumulator experiment on board *Rosetta* are in the mass range of $7.5 \times 10^{-8} - 1.6 \times 10^{-7}$ kg moving with velocities of 1–6 m s^{-1} (Della Corte et al. 2015). Analysis of the dust particles collected by *Rosetta* COSIMA revealed no indication of volatiles carried by the dust particles (Schulz et al. 2015).

It is interesting that the submicron particle flux coming from the solar direction exceeds that from the direction to the comet's nucleus by a factor of 3 (Della Corte et al. 2015). It suggests that charging, and the Lorentz force, may have a significant effect on dust particle dynamics, which can be especially important for small particles.

Under the commonly accepted paradigm, the sunlight heating is a dominant factor determining gas- and dust-ejection rates from the nucleus' surface, which makes them a function of the sub-solar angle and properties of the surface (such as the amount of volatiles available for injection into a coma) (e.g. Tenishev, Combi & Davidsson 2008; Belton 2013). It is also commonly assumed that a dust source rate is proportional to that of gas (e.g. Tenishev, Combi & Rubin 2011). In an analysis by Clark et al. (2004), they have suggested that other processes such as thermal stress, internal gas pressure, or turbulence can be involved in dust release into a coma.

The sunset jet recently observed with OSIRIS on board *Rosetta* has questioned the validity of this paradigm. As such, Shi et al. (2016) have suggested that a thermal lag in the nucleus uppermost subsurface layer can sustain the sunset jets.

3 MODELLING APPROACH

The collision regimes in a cometary coma vary in the range starting from collision dominated in the innermost vicinity of a comet's nucleus at small heliocentric distances through a transition one to the fully collisionless. Consequently, a coma modelling approach needs to be valid under all these regimes.
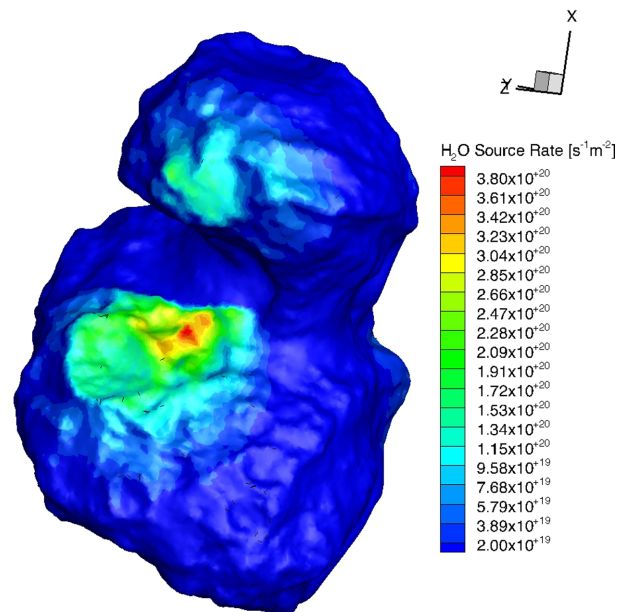

Figure 1. Water vapour source rate distribution inferred from *Rosetta* VIRTIS-M observation I1_00387442903 by Fougere et al. (2016), and used in the modelling work presented in this paper.

Based on solving the Boltzmann equation, the Direct Simulation Monte Carlo (DSMC) method became a commonly accepted approach for the modelling of gas and dust in the cometary coma environment. A need to analyse and interpret *Rosetta*'s observations has noticeably increased the intensity of cometary coma modelling efforts that are particularly focused on comet 67P/Churyumov–Gerasimenko. Some of the recent modelling work is described by, for example, Tenishev et al. (2008), Tenishev et al. (2011), Soja et al. (2015), Thomas et al. (2015), Moreno et al. (2013, 2014), Pozuelos et al. (2014), Gundlach et al. (2015), Lin et al. (2016), and Marschall et al. (2016).

The analysis presented in this paper has been performed using the Adaptive Mesh Particle Simulator model, which is a Monte Carlo code built within the frame of the DSMC methods. A detailed description of the code is presented by, for example, Tenishev et al. (2008) and Tenishev et al. (2013).

3.1 Neutral gas in a cometary coma

Gas- and dust-ejection rates from a comet's nucleus are mainly determined by an energy balance and heat transfer in the uppermost layer of the nucleus, which makes them highly dependent on the comet's heliocentric distance. As pointed by, for example, Davidsson & Gutiérrez (2006), they also depend on the surface illumination conditions and will be significantly different on the day- and night-side of the nucleus, and even on the day-side hemisphere during non-illuminated periods caused by the complex nucleus shape and self-shadowing.

The water vapour nucleus surface source distribution used in this analysis is presented in Fig. 1. This water vapour source has been adopted from our previous work by Fougere et al. (2016). The water vapour column density calculated with that volatile source and that observed by *Rosetta* VIRTIS-M (Migliorini et al. 2016) are compared in Fig. 2. The local water vapour source rate has been calculated using a combination of the surface illumination and the surface activity distribution to account for the non-uniformity of
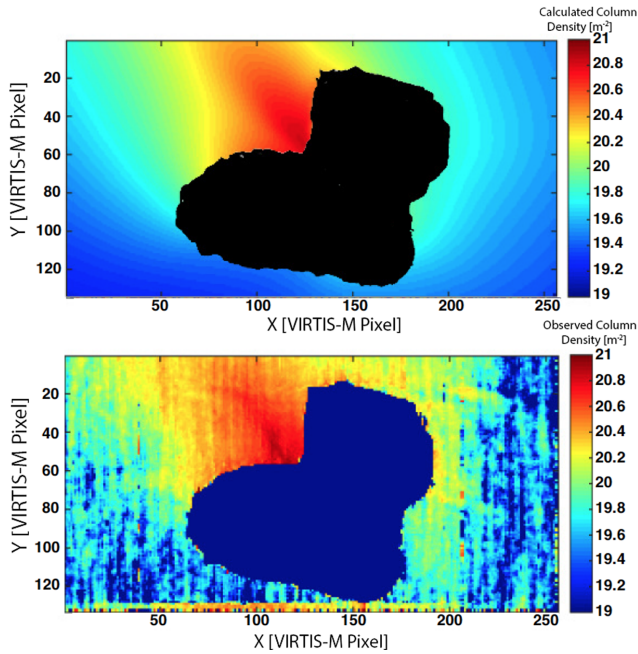
Figure 2. Comparison of the H_2O column density (m^{-2}) map observed by *Rosetta* VIRTIS-M [observation I1_00387442903, Migliorini et al. (2016)] with that from our previous kinetic modelling of the coma by Fougere et al. (2016). The surface distribution of the water vapour flux used in the analysis presented in this paper, and this figure are adapted from Fougere et al. (2016). Modelled column density is shown in the top panel and the observed one is shown in the bottom panel. *X*- and *Y*-axes represent the instrument pixel grid.

the surface outgassing. Due to the variability of the orientation of the comet's nucleus relative to the Sun, the local illumination is inherently time-dependent. This results in a temporal variability of the source rate. To account for this variability, we have recalculated the water vapour source for each of the four analysed VIRTIS-M observations.

3.2 Dust in a cometary coma

For purposes of the analysis presented in this paper, we have performed a coupled modelling of the gas and dust populating the coma of comet 67P/Churyumov–Gerasimenko.

Motion of the dust particles in the vicinity of the nucleus is mainly determined by a combination of the drag and gravity forces. In our modelling, we have calculated a dust particle location by integrating the equation of motion

$$\frac{d\mathbf{v}_g}{dt} = \frac{1}{m_g} \left[\pi a^2 \frac{C_D}{2} \rho (\mathbf{v} - \mathbf{v}_g) |\mathbf{v} - \mathbf{v}_g| - F_g \right], \tag{1}$$

where $m_g = 4/3 \pi a^3 \rho_g$ is the mass of a dust particle, C_D is a drag coefficient, F_g is the gravity force acting upon a particle, $\mathbf{v}$ is the bulk velocity of the ambient gas in the coma, $\mathbf{v}_g$ is the velocity of a spherical dust particle with radius a, and ρ and ρ_g are the mass density of the ambient gas and dust particles, respectively. In such an approximation, the equation of motion neglects the rotation of the nucleus, which may be seen as a curvature of the dust flow. Since VIRTIS-M dust brightness images that we analysed in this study have no obvious curved features resulting from this rotation, its effect was neglected. A more detailed analysis of dust particle trajectories in the coma of comet 67P/Churyumov–Gerasimenko

was done by, for example, Kramer & Noack (2016), who have accounted for the nucleus rotation in their modelling of the dust transport.

Here, we have explicitly assumed a spherical shape of the simulated dust particles. More complex non-spherical particles are considered by, for example, Fulle et al. (2015a). Such models involve additional unconstrained parameters describing shapes and orientations of the particles. In order to reduce the number of such parameters, we have limited our analysis by considering only spherical dust particles.

The most important advantage of a kinetic dust model employed in our analysis as opposed to a fluid one is that dust particle trajectories can cross in the coma because of the geometrical complexity of the nucleus, and can return to its surface in regions where the gas flux is low.

Because of the geometrical complexity of comet 67P/Churyumov–Gerasimenko's nucleus, a gravity acceleration vector needs to be calculated numerically by taking the following integral:

$$\mathbf{a}_g = -G \int_V \frac{\rho_n}{r^2} \frac{\mathbf{r}}{|\mathbf{r}|} dV, \tag{2}$$

where $\mathbf{a}_g$ is the gravity acceleration of a dust particle, $\mathbf{r}$ is the location of the nucleus volume element dV relative to the particle, G is the gravity constant, and ρ_n is the mass density of the nucleus (e.g. Fougere et al. 2013; Fougere 2014). In our analysis, we have assumed a nucleus mass density of $\rho_n = 430 \, \text{kg} \, \text{m}^{-3}$, which is consistent with that assumed by Kelley et al. (2013), and Thomas et al. (2015).

It is not realistic to recalculate the gravity acceleration as defined by equation (2) for each particle on each simulation time step. Instead, we have precalculated gravity-acceleration vectors at the centres of all computational cells, and then interpolated those to a particle location to get the acceleration acting upon a particle during the course of a simulation.

Usually, a drag coefficient, C_D, is determined assuming a free molecular flow, isothermal dust grains, and a diffuse reflection of the gas molecules on the grains:

$$C_D = \frac{2s^2 + 1}{s^3 \sqrt{\pi}} \exp(-s^2) + \frac{4s^4 + 4s^2 - 1}{2s^4} \text{erf}(s) + \frac{2\sqrt{\pi}}{3s} \sqrt{\frac{T_d}{T_g}}, \tag{3}$$

where $s = |\mathbf{v}_g - \mathbf{v}_d| / \sqrt{2k_B T_g / m_g}$, and T_d and T_g are the temperatures of a dust grain and the ambient gas, respectively (e.g. Crifo et al. 2005). For purposes of the practical calculations, the drag coefficient can be approximated by a constant $C_D = 2$, which adequately describes the interaction between gas and dust in conditions that exist in cometary comae (e.g. Tenishev et al. 2011; Della Corte et al. 2015).

We have used a dust mass density of $\rho = 1000 \, \text{kg} \, \text{m}^{-3}$. In our analysis of the dust brightness maps, we have experimented with the power-law index varying in the range between -5 and -2. We have found that the calculated dust brightness agreed best with the observed images when the power-law index is -2.5, which is consistent with that used by Marschall et al. (2016) in their analysis of *Rosetta* OSIRIS dust images. Simulated dust particle radii vary in the range of $10^{-7} < a < 10^{-3}$ m. Only those particles that can be lifted according to the balance between the local gravity at the surface and the local drag force were ejected into the coma.
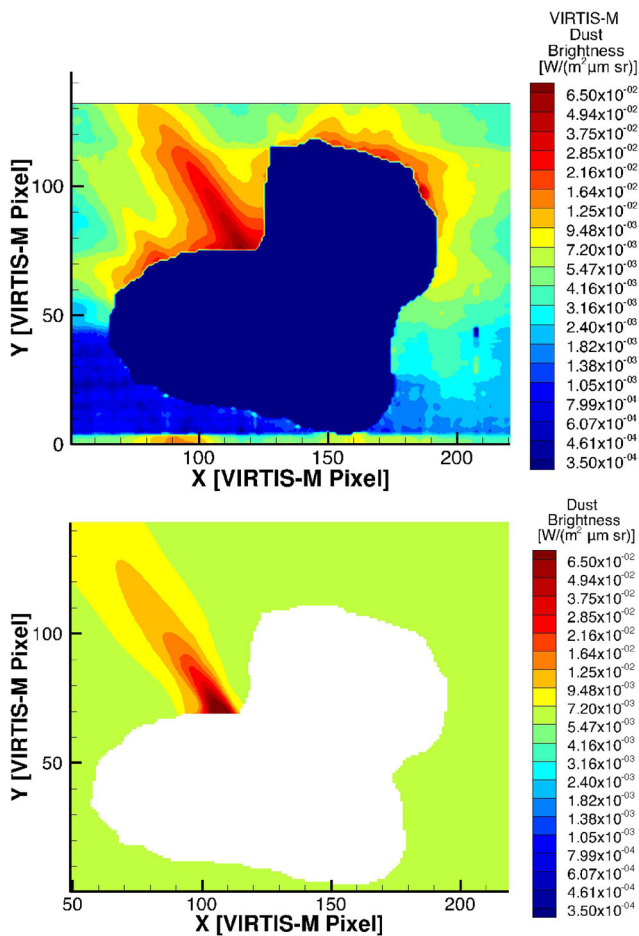
Figure 3. Comparison of the cometary dust brightness map observed by *Rosetta* VIRTIS-M [observation I1_00387442903 taken on 2015-04-12T07:14:00, Migliorini et al. 2016] with that from our kinetic modelling of gas and dust in the coma of comet 67P/Churyumov–Gerasimenko. The observed brightness map is shown in the top panel, and the modelled one is shown in the bottom panel. *X*- and *Y*-axes represent the instrument pixel grid.

Figure 4. Comparison of the cometary dust brightness map observed by *Rosetta* VIRTIS-M [observation I1_00387379010 taken on 2015-04-11T13:40:00, Migliorini et al. 2016] with that from our kinetic modelling of gas and dust in the coma of comet 67P/Churyumov–Gerasimenko. The observed brightness map is shown in the top panel, and the modelled one is shown in the bottom panel. *X*- and *Y*-axes represent the instrument pixel grid.

3.3 Fitting of the model to the VIRTIS-M dust brightness observations

We have inferred the location and source rate of the jet in two stages. First, we have simulated the dusty coma assuming a constant dust-to-gas mass ratio. During this phase, we not only have calculated macroscopic parameters of the dust flow (such as density or bulk velocity), but also have saved about 300 000 trajectories of individual simulated dust particles. With these, we have calculated the dust brightness as it would be seen from the spacecraft, and used the latter to infer the location and source rate of the jet. Then the simulation has been repeated with the inferred dust source to verify the consistency of the calculated dust brightness obtained by analysing the saved individual trajectories with that calculated with the full-scale dusty coma simulation.

4 MODEL RESULTS AND COMPARISON WITH OBSERVATIONS

Modelling performed as a part of this work was used to infer a mass source rate, and the location of the origin of the dust jet observed
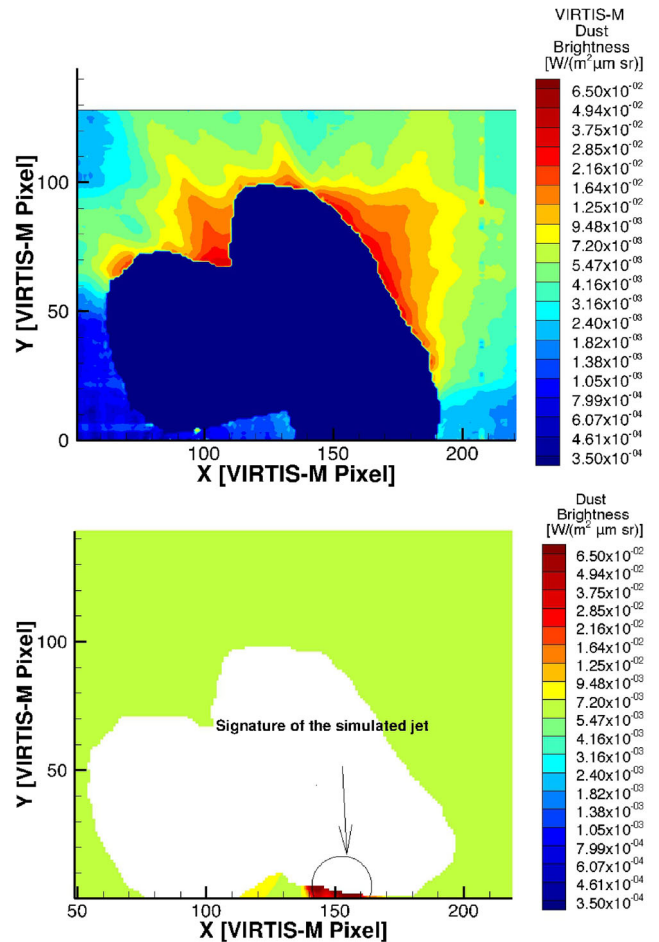
by *Rosetta* VIRTIS-M on 2015 April 12 (2015-04-12T07:14:00) (Migliorini et al. 2016).

We have calculated the dust brightness as it would be seen by *Rosetta* using the simulated cometary dust distribution, and compared that with the coma brightness observed by *Rosetta* VIRTIS-M. The modelled dust brightness is obtained by taking the following integral:

$$I(\lambda) = F(\lambda) \int n(\boldsymbol{r}) \sigma_g q_s(\lambda) \frac{p(g)}{4\pi} \mathrm{d}s, \qquad (4)$$

where $F(\lambda)$ is the solar flux at a comet's location, $n(\boldsymbol{r})$ is a dust number density, σ_g is the geometrical cross-section of a dust grain, $q(\lambda)_s$ is a scattering efficiency, and $p(g)$ is a normalized phase function (e.g. Kolokolova et al. 2004; Fink & Rubin 2012; Fink & Rinaldi 2015). In this work, scattering efficiency, $q_s(\lambda)$, was calculated assuming 'Halley-dust' particles with the ice-to-dust ratio of 0.05, and porosity of 0.83 (Nagdimunov et al. 2014).

The analysed VIRTIS-M image is made at a wavelength of 1.09 μm. Following the calibration procedure accepted by the *Rosetta* VIRTIS team, we have assumed a solar flux of $F(1.09\,\mu\mathrm{m}) = 586.86\,\mathrm{W\,m^{-2}\,\mu m^{-1}}$ at 1 au. The comet was
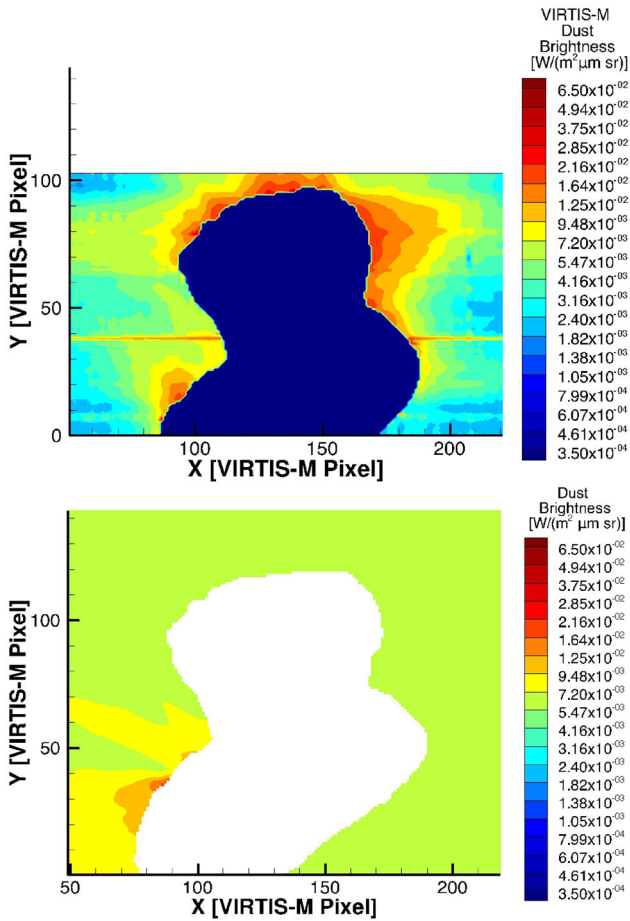
Figure 5. Comparison of the cometary dust brightness map observed by *Rosetta* VIRTIS-M [observation I1_00387481450 taken on 2015-4-12T17:57:00, Migliorini et al. 2016] with that from our kinetic modelling of gas and dust in the coma of comet 67P/Churyumov–Gerasimenko. The observed brightness map is shown in the top panel, and the modelled one is shown in the bottom panel. *X*- and *Y*-axes represent the instrument pixel grid.

Figure 6. Comparison of the cometary dust brightness map observed by *Rosetta* VIRTIS-M [observation I1_00387554894 taken on 2015-4-13T14:21:00, Migliorini et al. 2016] with that from our kinetic modelling of gas and dust in the coma of comet 67P/Churyumov–Gerasimenko. The observed brightness map is shown in the top panel, and the modelled one is shown in the bottom panel. *X*- and *Y*-axes represent the instrument pixel grid.

located at a heliocentric distance of 1.88 au on 2015 April 12. Scaled to that heliocentric distance, the solar flux is $F(1.09\,\mu\text{m})|_{1.88\text{au}} = 166\,\text{W}\,\text{m}^{-2}\,\mu\text{m}^{-1}$, which was used for further calculation of the dust brightness, as defined in equation (4).

In this work, we have focused our analysis on the observed jet itself, leaving the global distribution of the dust cloud imaged by *Rosetta* VIRTIS-M (Fig. 3) out of the scope of the investigation. For this reason, we split the observed dust brightness into background dust cloud and dust jet contributions. We estimate the former to be about 0.007 W/($\text{m}^2\,\mu\text{m}$ sr) from the image in Fig. 3. Fitting of the calculated dust brightness to that observed by *Rosetta* VIRTIS-M suggests a total mass source rate of 1.9 kg s^{-1} during the lifetime of the observed jet.

To compare the dust brightness maps observed on 2015-04-11T13:40:00 (observation I1_00387379010), 2015-04-12T17:57:00 (observation I1_00387481450), and 2015-04-13T14:21:00 (observation I1_00387554894) with our model, we have simulated the dusty coma for each of the observation times independently with the water vapour source as described in Section 3.1, and assuming the dust source location and strength as inferred from the jet image taken on 2015-04-12T07:14:00 (observation I1_00387442903). Simulated and observed brightness maps
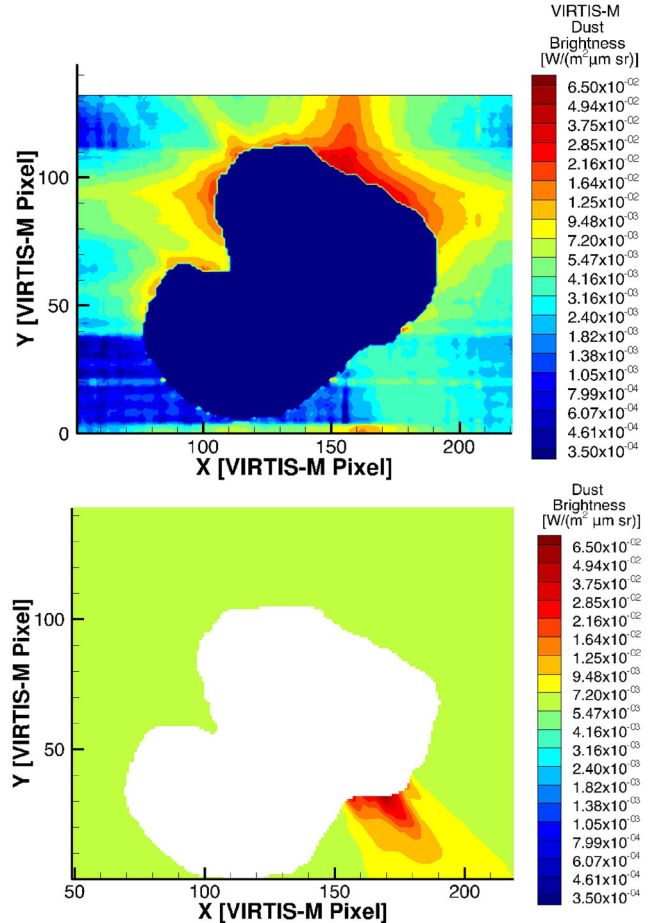
are presented in Figs 4–6. These indicate a temporal variability of the jet and suggests that it has a lifetime of at least 10 h.

It is important to note that we have neglected the rotation of the nucleus. Therefore, the calculations presented are the steady-state solutions for both gas and dust performed at the illumination conditions and the nucleus orientation with respect to the Sun that corresponds to each of the analysed observations individually. As pointed out by Marschall et al. (2016), such a simplification is adequate for calculating the gas and dust brightness in the coma.

As part of the presented analysis, we have determined footprints of the dust particle trajectories that could contribute to the observed jet. These footprints are concentrated outside of the area of the maximum gas production, and located in the Seth region, as shown in Figs 1 and 7.

We estimate the surface area of the dust source region of about 1.3 per cent of the total nucleus surface area. Taking the total dust-to-gas ratio of 6, and a gas production rate at the time of VIRTIS-M observation I1_00387442903 from Fougere et al. (2016), the total dust mass source rate would be of about 71 kg s^{-1} and, consequently, the fraction of the dust ejected into the jet of 2.6 per cent.
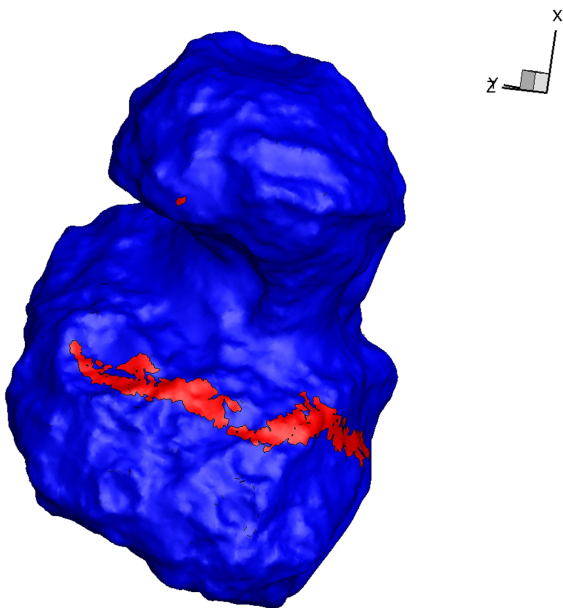
Figure 7. Inferred trajectory footprint location of those particles that could contribute to the jet brightness shown in Fig. 3. The footprints, marked in red, are concentrated in an area outside of the maximum watersource rate region shown in Fig. 1. The inferred trajectory footprint location area is consistent with that of the active pits in the Seth region, as determined by Vincent et al. (2015).

5 SUMMARY

In this paper, we present results of our analysis of the dust brightness image acquired by *Rosetta* VIRTIS-M on 2015 April 12. The main focus of this work is determining the location and dust mass source rate that is needed to explain the observed dust brightness of the jet. The analysis was performed by means of a coupled kinetic modelling of gas and dust populating the coma of comet 67P/Churyumov–Gerasimenko, and comparing the calculated dust brightness with that observed by *Rosetta* VIRTIS-M. This analysis suggests a dust mass source rate of 1.9 kg s^{-1} at the location of the jet origin, which is needed to reproduce the observed dust brightness.

Signatures of the simulated dust jet are present in two (Figs 3 and 5) out of four VIRTIS-M images (Figs 3–6), which allows us to conclude that this is a time-varying jet with a lifetime of at least of 10 h.

The most important result of this study is that the nucleus surface footprints of the dust particle trajectories that could populate the jet are concentrated outside of the maximum gas production area, which is located close to the terminator line, as suggested by Fougere et al. (2016). The locations of these footprints are shown in Fig. 7. This suggests that there is no simple proportionality relation between gas and dust production rates, which raises the question of the nature of the dust-release mechanism that produces jets in a region outside of the area with the highest gas production rate. The inferred footprint location area is consistent with that of the active pits in the Seth region, as determined by Vincent et al. (2015).

REFERENCES

Belton M. J., 2013, Icarus, 222, 653
Bockelée-Morvan D., Crovisier J., 1987, Proc. Int. Symp., Diversity and Similarity of Comets. European Space Agency, Paris, p. 235
Burch J. L., Gombosi T. I., Clark G., Mokashi P., Goldstein R., 2015, Geophys. Res. Lett., 42, 6575
Clark B. C., Green S. F., Economou T. E., Sandford S. A., Zolensky M. E., McBride N., Brownlee D. E., 2004, J. Geophys. Res., 109, E12S03
Combi M., 1996, Icarus, 123, 207
Combi M. R., Smyth W. H., 1988, ApJ, 327, 1026
Crifo J., Loukianov G. A., Rodionov A. V., Zakharov V. V., 2005, Icarus, 176, 192
Davidsson B. J. R., Gutiérrez P. J., 2006, Icarus, 180, 224
Della Corte V. et al., 2015, A&A, 583, A13
Fink U., Rinaldi G., 2015, Icarus, 257, 9
Fink U., Rubin M., 2012, Icarus, 221, 721
Fougere N., 2014, PhD thesis, Univ. Michigan
Fougere N., Combi M., Rubin M., Tenishev V., 2013, Icarus, 225, 688
Fougere N. et al., 2016, A&A, 588, A134
Fulle M. et al., 2015a, A&A, 583, A14
Fulle M. et al., 2015b, ApJ, 802, L12
Gundlach B., Blum J., Keller H. U., Skorov Y. V., 2015, A&A, 583, A12
Kelley M. S., Lindler D. J., Bodewits D., A'Hearn M. F., Lisse C. M., Kolokolova L., Kissel J., Hermalyn B., 2013, Icarus, 222, 634
Kolokolova L., Hanner M. S., Levasseur-Regourd A.-C., Gustafson B. Å. S., 2004, in Festou M, Uwe Keller H., Weaver H. A., eds, Comets II. University of Arizona Press, Tucson, AZ, p. 577
Kramer T., Noack M., 2016, ApJ, 813, L33
Lara L. M. et al., 2015, A&A, 583, A9
Lin Z.-Y. et al., 2015, A&A, 583, A11
Lin Z.-Y. et al., 2016, A&A, 588, L3
Marschall R. et al., 2016, A&A, 589
Migliorini A. et al., 2016, A&A, 589, A45
Moreno F., Cabrera-Lavers A., Vaduvescu O., Licandro J., Pozuelos F., 2013, ApJ, 770, L30
Moreno F. et al., 2014, AJ, 791, 118
Nagdimunov L., Kolokolova L., Wolff M., A'Hearn M. F., Farnham T. L., 2014, Planet. Space Sci., 100, 73
Pozuelos F. J. et al., 2014, A&A, 571, A64
Rotundi A. et al., 2015, Science, 347
Schulz R. et al., 2015, Nature, 518, 216
Shi X. et al., 2016, A&A, 586, A7
Skorov Y., Blum J., 2012, Icarus, 221, 1
Soja R. H. et al., 2015, A&A, 583, A18
Tenishev V., Combi M., Davidsson B., 2008, ApJ, 685, 659
Tenishev V., Combi M. R., Rubin M., 2011, ApJ, 732
Tenishev V., Rubin M., Tucker O. J., Combi M. R., Sarantos M., 2013, Icarus, 226, 1538
Thomas N. et al., 2015, A&A, 583, A17
Vincent J.-B. et al., 2015, Nature, 523, 7558

This paper has been typeset from a TEX/LATEX file prepared by the author.